Some effects of the moisture distribution in the subcloud layer on the thermal structure of a mature severe thunderstorm

By Y. J. LIN and H. J. HWANG, *Department of Earth and Atmospheric Sciences, Saint Louis University, St. Louis, Mo., USA*

(Manuscript received July 18, 1973; revised version January 10, 1974)

ABSTRACT

A four-layer, non-entraining axial-symmetric, steady-state model of a severe thunderstorm with a rotating updraft is used to study some effects of the low-level moisture fields on the thermal and dynamical structure of the storm. This model represents the third in a series of three models which have been produced at Saint Louis University. It differs from the other two which were developed by Lin & Martin (1971, 1972) by the fact that moisture becomes a specified input parameter rather than a deduced one. The three models have been checked to assure their internal consistency so that any one of them can be used to generate a common field of gridded variables depending upon the nature of the observed evidence at hand.

The selective mix of observed and generated data within the updraft of the modelled storm, provided by the particular model of this respect, was used to evaluate (1) vertical velocities from the mass continuity equation, (2) moisture distribution in the subcloud layer from the continuity equation for water vapor, (3) the field of pressure based on the radial equation of motion, (4) the temperature field using the thermodynamic energy equation, and (5) moisture fluxes, latent heat releases and static energies utilizing the data obtained from (1) through (4). The results indicate that a substantial percentage of the latent heat releases within a storm must be confined to the lower portion of the atmosphere in order for a warm-core center to be maintained. The low-level relative humidity of the embedding environment was found to be a strong indicator of severe thunderstorm development. The "static energy differentials" between a storm and its environment are compared for a modelled and observed storm to illustrate certain agreements among the modelled and natural physical processes in operation.

1. Introduction

The development and maintenance of severe thunderstorms are influenced by transports of momentum, heat and moisture by eddies in the atmospheric boundary layer (e.g., Sasaki, 1966; Bonner, 1966; Newman, 1972). Consequently, various combinations of these parameters are employed to predict the probability of severe weather occurrences (U.S. Weather Bureau, 1965; Miller, 1972). For example, Sasaki et al. (1967) found moisture fluxes and divergences to relate quite well to areas of convective activity and severe weather occurrences. These two-particular boundary-layer phenomena were also successfully used to parameterize latent heat releases in tropical storm research by Kuo (1965) and in pertaining to midlatitude severe convective storms by Hudson (1971).

Hudson found vigorous cumulus convection to be associated, in general, with well-defined axes of horizontal moisture convergence. These results were collaborated by the study of Ninomiya (1971) on the interaction between the meso-scale convective storm and its environment. The importance of vertical moisture fluxes from the subcloud layer into the updraft of the severe thunderstorm has also been indicated by many observational studies, e.g., Fankhauser (1965, 1966), Newton (1966), Auer & Marwitz (1968). The magnitude of these fluxes was calculated by Fankhauser (1966) to be on the order of $28 \times 10^9 \varrho \sec^{-1}$ for a hailstorm in Oklahoma. Magnitudes of approximately 8.8×10^9 g sec^{-1} were found by Newton (1966) and 3.1×10^9 g sec^{-1} by Auer & Marwitz (1968). These values are approximately one or two orders of magnitude greater than those found for the "air mass" thunderstorm (see Braham, 1952).

The difficulties and hazard of making measurements within intense convective cells have impeded the direct observational assessments of the relative roles played by each of the various physical processes occurring within them. Hence, we propose to make these assessments by introducing observed peripheral data as boundary conditions into our diagnostic severe thunderstorm modelling research. The model to be presented uses such information to formulate the wind-component parameters and to specify the boundary conditions for moisture, temperature and pressure. Fields of vertical velocity, temperature and pressure internal to the storm, which are consistent with those more readily observed evidences in the outer reaches of the severe thunderstorm, are then generated by the model. These are used to study some effects of the low-level moisture fields on the thermal and dynamical structure of the modelled storm.

2. The model

A four-layer, non-entraining, axial-symmetric, steady-state model of a severe thunderstorm with a rotating updraft is devised. The layer which ranges from the surface ($z = 0$) to a height of $z_b = 1$ km is taken to represent the atmospheric boundary layer beneath the cloud base. The main body of the storm's updraft configuration is assumed to extend from the top of this layer to a height of 15 km. It is defined by three equally spaced segments (see Fig. 1). The outer boundary of the storm's updraft, r_{lb}, is assumed to be 10 km.

The model requires analytically formulated radial and tangential velocities, u and v. Values of specific humidity within the main body of the storm's updraft configuration, q, are specified in terms of "partition ratio" of condensed water vapor (to be discussed in Section 3.2). The surface temperature, T_0, and specific humidity values, q_0, are inferred from observational data near the ground. The vertical velocity, w_b, at $z = z_b$ is deduced from the horizontal wind fields using the formula patterned after the study of Charney & Eliassen (1964). In the subcloud layer of the storm, pressure p_r, and moisture q_r, at $r = r_{lb}$ are inferred from sounding data.

The model uses these input values to calculate the following variables in the storm's updraft configuration:

1. Vertical velocity based on considerations involving the mass continuity equation;
2. temperature using the thermodynamic energy equation combined with equations of radial and vertical motion; and
3. pressure based on the radial equation of motion.

In addition, the spatial distribution of water vapor within the subcloud layer ($0 \leqslant z_s \leqslant z_b$) is obtained by integrating the continuity equation for water vapor inward from the $r = r_{lb}$ to the center $r = 0$. This treatment will be detailed in Section 3. These data are in turn used to calculate moisture fluxes, latent heat releases and static energies throughout the main body of the modelled storm.

Before proceeding with the discussion of these calculations, some of the more pertinent modelling assumptions will be justified. The steady-state assumption is based on evidences supplied by the studies of Browning & Ludlam (1962), Donaldson (1962), Browning & Donaldson (1963), Auer & Sand (1966), Schlesinger (1971) and Fankhauser (1971). They reported that severe thunderstorms often retain quasi-invariant shapes and sizes for periods extending as long as two hours.

The assumption of non-entrainment is based, in part, on the works of Bates (1961), Fujita & Byers (1962) and Malkus & Williams (1963). These studies suggest that the effects of lateral entrainment are small, by comparison with the other processes being considered, during the mature stage of the storm's life cycle. Recent evidence which runs somewhat counter to this assumption has been supplied by Brown & Crafford (1972). They found that the storm cell is neither sufficiently rigid to divert the winds around it nor amorphous to permit every part of the cloud structure to yield separately to the wind force exerted on it. On the other hand, Baxter (1971) showed the updraft configuration in a severe thunderstorm to be intimately related to the strength of an accompanying

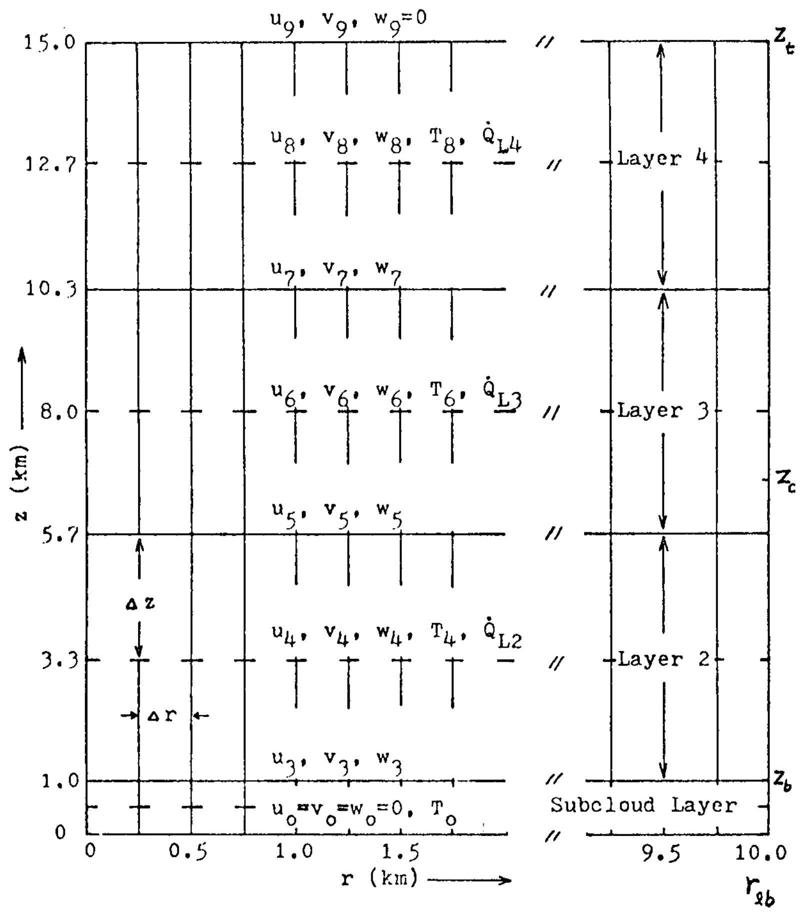

Fig. 1. The four-layer model of a severe thunderstorm. In layers 2, 3 and 4, the specified variables are radial velocity (u), tangential velocity (v) and specific humidity (q), and the calculated variables are vertical velocity (w), temperature (T) and pressure (P).

"forced" downdraft arising from the evaporative cooling of entrained dry environmental air into the rear portion of the storm cell. He reasoned that the sharp temperature contrast between the "forced" downdraft and the updraft portions of the severe thunderstorm would provide a barrier to mixing between them. Hence, an amorphous downdraft does not automatically preclude the use of a non-entrainment assumption in the updraft portion when the latter is being considered as a separate entity.

The assumption that certain severe thunderstorms rotate is supported by Bates (1961), Browning (1965*a*, *b*), Stein & Rhyne (1962), Fitzgerald & Valvocin (1964), Koschielski (1967), Doswell & Tegtmeier (1972), Fujita & Grandoso (1968), and Charba & Sasaki (1971). The axial-symmetric assumption is difficult to justify since it automatically and completely isolates the storm from its environment. Its employment, at this time, lies in our belief that many gross characteristics of the storm, which can be captured when that assumption is invoked, are yet to be uncovered. We did not choose, therefore, to complicate the mathematica]representations until their simple forms have been more fully exploited.

The simplified governing equations for the storm model in cylindrical coordinates (r, ϕ, z, t) are:

Table 1. *List of symbols*

c_p	specific heat for dry air at constant pressure
E_s	"static energy" per unit mass
f	Coriolis parameter
g	acceleration of gravity
K_m^H	horizontal momentum exchange coefficient
K_m^z	vertical momentum exchange coefficient
K_w^H	horizontal eddy diffusion coefficient for water vapor
K_w^z	vertical eddy diffusion coefficient for water vapor
L	latent heat of condensation
l_i	"partition ratio" of water vapor condensed in the ith layer
M_z	area mean of vertical moisture flux density
P	pressure
p_r	pressure in the reference atmosphere
$\dot{Q}$	rate of change of diabatic heat per unit mass
$\dot{Q}_L$	rate of change of latent heat per unit mass
q	specific humidity
q_b	specific humidity at the top of the subcloud layer
q_r	specific humidity in the reference atmosphere
q_s	saturation specific humidity
R_d	gas constant of dry air
r	radial distance (positive outward)
r_{lb}	outer boundary of the storm's updraft
Δr	radial grid distance
T	temperature (in Kelvin degree)
T_r	temperature at the reference atmosphere
u	radial velocity (positive outward)
v	tangential velocity (positive counterclockwise)
w	vertical velocity (positive upward)
w_b	w at $z = z_b$
z	height
z_b	height of the subcloud layer
Δz	vertical grid distance
α	specific volume
γ	temperature lapse rate
γ_d	dry-adiabatic lapse rate (= 10°C km^{-1})
γ_m	moist-adiabatic lapse rate (= 6.4°C km^{-1})
ϱ	density
$\bar{\varrho}$	density in the reference atmosphere

(*a*) Radial equation of motion

$$u\frac{\partial u}{\partial r} + w\frac{\partial u}{\partial z} - v\left(f + \frac{v}{r}\right) + R_d T\frac{\partial \ln P}{\partial r} = K_m^H\left(\frac{\partial^2}{\partial r^2} + \frac{1}{r}\frac{\partial}{\partial r} - \frac{1}{r^2}\right)u + K_m^z\frac{1}{\bar{\varrho}}\frac{\partial}{\partial z}\left(\bar{\varrho}\frac{\partial u}{\partial z}\right) \tag{1}$$

(*b*) Tangential equation of motion

$$u\frac{\partial v}{\partial r} + w\frac{\partial v}{\partial z} + u\left(f + \frac{v}{r}\right) = K_m^H\left(\frac{\partial^2}{\partial r^2} + \frac{1}{r}\frac{\partial}{\partial r} - \frac{1}{r^2}\right)v + K_m^z\frac{1}{\bar{\varrho}}\frac{\partial}{\partial z}\left(\bar{\varrho}\frac{\partial v}{\partial z}\right) \tag{2}$$

(*c*) Vertical equation of motion

$$u\frac{\partial w}{\partial r} + w\frac{\partial w}{\partial z} + g + R_d T\frac{\partial \ln P}{\partial z} = 0 \tag{3}$$

(*d*) Mass continuity equation

$$\bar{\varrho}\frac{\partial (ru)}{r\partial r} + \frac{\partial(\bar{\varrho}w)}{\partial z} = 0 \tag{4}$$

(*e*) Thermodynamic energy equation

$$c_p\left[u\frac{\partial T}{\partial r} + w\frac{\partial T}{\partial z}\right] - R_d T\left[u\frac{\partial \ln P}{\partial r} + w\frac{\partial \ln P}{\partial z}\right] = \dot{Q}_L \tag{5}$$

(*f*) Continuity equation for water vapor (applied to the subcloud layer only)

$$\frac{1}{r}\frac{\partial}{\partial r}[\bar{\varrho}uq^*r] + \frac{\partial}{\partial z}[\bar{\varrho}q^*w] = \frac{\bar{\varrho}K_w^H}{r}\frac{\partial}{\partial r}\left(r\frac{\partial q^*}{\partial r}\right) + K_w^z\frac{\partial}{\partial z}\left(\bar{\varrho}\frac{\partial q^*}{\partial z}\right) \tag{6}$$

Here q^* denotes the specific humidity in the subcloud layer ($0 \leqslant z_s \leqslant z_b$), and the other symbols are described in Table 1.

The frictional terms on the right of eqs. (1) and (2) are parameterized in accordance with the studies of Ogura (1963), Orville & Sloan (1970), Rothensal (1970*a*, *b*), Takeda (1971), and Lin & Martin (1972). Mixing length considerations were used to approximate the lateral coefficient of eddy viscosity by the expression $K_m^H \sim L'v'$ where L' is the scale length of the eddy and v' is the magnitude of the wind gusts due to the eddies. The data of Rhyne & Steiner (1964) and Ackerman (1967) indicate that K_m^H ranges between 9×10^7 and 35×10^7 cm^2 sec^{-1} for convective clouds. Ogura (1963) estimates its magnitude to be approximately 10^7 cm^2 sec^{-1} for shallow cumulus clouds.

Corresponding magnitudes for the vertical

Table 2. *Magnitudes of momentum and water vapor exchange coefficients (in m^2 sec^{-1}) used by other researchers*

Investigator	K_m^H	K_m^z	K_w^H	Δr (km)	Δz (km)	r_{max} (km)	z_{max} (km)	Remarks
Lin & Martin (1972)	4×10^3	100		0.25	0.25	10	15	Severe storm
Liu & Orville (1969)	40	40	40	0.1	0.1	7	3.5	Shallow cumulus
	2	2	2	0.01	0.01	7	3.5	Shallow cumulus
Ogura (1963)	40	40	40	0.1	0.1	3	3	Shallow cumulus
	10^3	10^3	10^3					Suggested for thunderstorm
Orville & Sloan (1970)	80	80	80	0.1	0.1	10	10	Rainstorm
	4	4	4	0.01	0.01	10	10	Rainstorm
Rosenthal (1970*a*)	10^4	10		20	100^a	440	100^a	Tropical cyclone
(1970*b*)	10^3	0–10	10^4	10	100^a	440	100^a	Tropical cyclone
Takeda (1971)	500	500	500	1	0.5	25	10	Precipitating convective cloud

[a] Units in mb.

component of eddy viscosity, K_m^z, are not as well documented. Rosenthal (1970*a*, *b*) used a value of 10^5 cm^2 sec^{-1} in his study of tropical cyclones. Those provided by other researchers are listed in Table 2. Values of $K_m^H = 4 \times 10^7$ cm^2 sec^{-1} and $K_m^z = 10^6$ cm^2 sec^{-1} were used in the model under discussion.

The horizontal wind fields were analytically expressed as follows. The tangential velocity representative of the severe thunderstorm is assumed to be separable into a radial dependent and a height dependent component:

$$v(r, z) = V_r(r)\, V_z(z) \tag{7}$$

The radial dependent function of the tangential velocity takes the form

$$V_r(r) = \frac{2 V_{max}\, r/r_m}{1 + (r/r_m)^2} \tag{8}$$

Here V_{max} is a constant corresponding to the maximum value of $V_r(r)$, and r_m is the radius at which V_{max} occurs. The non-dimensional height dependent function, $V_z(z)$, is calculated by solving the tangential equation of motion (2) together with the equation of continuity. The procedure used is similar to that introduced by Lin & Martin (1972).

The radial velocity is expressed by the formulation

$$u(r, z) = \frac{2 U_{max}(z)\, r/r_n^*(z)}{1 + [r/r_n^*[z)]^2} \tag{9}$$

The height dependent functions, $U_{max}(z)$ and $r_n^*(z)$, denote the maximum radial velocity at a given height z, and the radius at which U_{max} occurs. They are assumed to be

$$\left.\begin{aligned} U_{max}(z) &= -U_0^+ \cos\left(\frac{\pi z}{2 z_c}\right) \quad \text{for} \quad z > z_c \\ &= -U_0^- \cos\left(\frac{\pi z}{2 z_c}\right) \quad \text{for} \quad z \leqslant z_c \end{aligned}\right\} \tag{10}$$

and

$$r_n^*(z) = 1 + 0.5 \left[\frac{(z - z_c)}{z_c}\right]^2 \tag{11}$$

where z_c is the height which separates the inflow layers from the outflow ones. These expressions conform with the studies of Beebe & Bates (1955) and Fankhauser (1965, 1971) which demand a confluence of moist air in the lower troposphere and a diffluence aloft.

Values of 25 m sec^{-1} for V_{max}, 2 km for r_m, 5 m sec^{-1} for U_0^+, 3 m sec^{-1} for U_0^-, and 6.7 km for z_c best tune these analytical formulations to the observed evidence available to us for the outer extremities of the typical severe thunderstorm.

The mean density, $\bar{\varrho}(z)$, is assumed to be a function of height z only, since density, ϱ, varies much more slowly laterally than vertically and since its fluctuations are at least an

Table 3. *Values of temperature, T_r(°K), pressure, p_r(mb), and density, $\bar{\varrho}$(g cm^{-3}), for the reference atmosphere*

These were obtained from the average tornado-proximity sounding of Darkow (1969)

z (km)	T_r (°K)	p_r (mb)	$\bar{\varrho}$ (10^{-3} g cm^{-3}) $=p_r/R_d T_r$
0	301.3	1 013.0	1.172
0.5	296.0	954.6	1.124
1.0	293.0	898.7	1.069
3.3	277.0	671.7	0.845
5.7	262.0	493.5	0.656
8.0	245.0	355.7	0.506
10.3	226.4	250.9	0.386
12.7	213.0	172.6	0.282
15.0	209.5	115.4	0.191

order of magnitude smaller than its mean. The tornado-proximity data compiled by Darkow (1969) were used to establish these values (see Table 3).

The rate of change of diabatic heating, per unit mass, is approximated by a release of latent heat of condensation, i.e., $\dot{Q} \approx \dot{Q}_L$. This representation has been frequently used in the meteorological literature for tropical and extratropical storms and severe thunderstorms (e.g., Kuo, 1965; Rosenthal, 1970*a*, *b*, etc.). Since the portion of a severe thunderstorm which is occupied by the updraft configuration is generally at or near saturation, no provision is made in the model for the inclusion of evaporative processes. More detailed treatments of the $\dot{Q}_L$ term are provided in the Appendix and Section 3.2.

Lateral and vertical convergences of moisture fluxes are given by the terms on the left of eq. (6), and those on the right express the lateral and vertical components of turbulent mixing in the subcloud layer of the storm. Various estimates for K_w^H by other researchers are listed in Table 2. Values of 10^{10} cm^2 sec^{-1} for K_w^H and 10^6 cm^2 sec^{-1} for K_w^z were selected for our model based on numerous sensitivity experimentations and comparisons which we made between model-produced and independently derived values for the respective generated variables under consideration. These estimates appear to be somewhat larger than those used by the other investigations. It must be noted, however, that the magnitude of K_w^H and K_w^z is highly dependent on the specific model being considered as shown in Table 2.

3. Numerical experiments

Numerical experiments were performed using a 42×7 grid system. A horizontal grid spacing of 0.25 km and a vertical one of 2.33 km was used throughout the updraft. A somewhat finer vertical grid ($\Delta z = 0.1$ km) was used for the subcloud layer. A one-sided differencing method was employed to compute the advective terms and a centered-differencing scheme for the non-advective ones.

The following dependent variables within the storm's updraft configuration were calculated using the specified values of u and v and the known "partition ratio" of condensed water vapor to determine values of q:

3.1. *Vertical velocities $w(r, z)$*

The field of w was computed from the mass continuity equation (4) using the specified values of u from eqs. (9) to (11). The "frictionally-induced" vertical velocity, w_b, at the top of the subcloud layer, $z = z_b$, is used as a lower boundary condition for integrations. This quantity was calculated from the formula patterned after the study of Charney & Eliassen (1964), i.e.,

$$w_b(r, z_b) = \sqrt{\frac{K_m^z}{2f_0}}\, \zeta_s \sin 45° \tag{12}$$

where ζ_s is the surface vorticity, $f_0 = 10^{-4}$ sec^{-1} and $K_m^z = 1.4 \times 10^5$ cm^2 sec^{-1}.

Fig. 2 shows model-generated vertical profiles for w at $r = 0$, 1 and 2 km along with its radial distributions at $z = 1.5$ and 5.7 km. Note that values of approximately 7.5, 3.5 and 1.0 m sec^{-1} are given at $z = 1.5$ km for $r = 0$, 1 and 2 km, respectively. For comparative purposes, Marwitz (1972*d*) observed values range from 5.0 to 7.5 m sec^{-1} at the cloud base (approximately 1.5 km above the surface) using chaff-tracking techniques. Similarly, Henderson (1972) deduced values of approximately 5.0 m sec^{-1} at $z = 1.5$ km using NSSL's in-storm soundings. Thus, it appears that the modelled vertical velocity term, which is so critical to the transport of moisture, is moderately realistic.

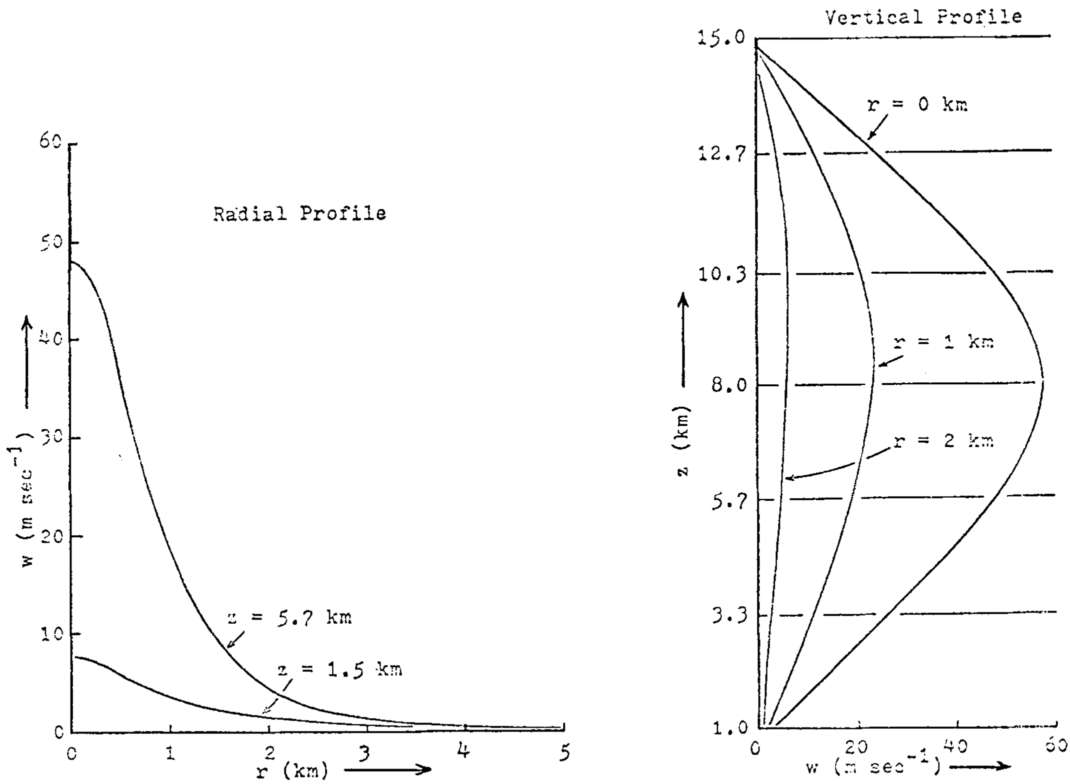

Fig. 2. Calculated vertical velocity profiles, w (m sec^{-1}), in the main body of a modelled storm.

3.2. *Temperatures* $T(r, z)$

The collective effects of cumulus convection are treated implicitly under the assumption that all the products of condensation precipitate out of the system. Thus, the release of latent heat by condensation in a unit mass of air per unit time can be written as

$$\dot{Q}_L = -L\frac{dq_s}{dt} \quad \text{when} \quad w > 0 \tag{13}$$

With the aid of eqs. (1) and (3), the thermodynamic energy equation (5) becomes

$$w\frac{\partial T}{\partial z} = \frac{\dot{Q}_L}{c_p} - u\frac{\partial T}{\partial r} + \frac{u}{c_p}G_1(r, z) + \frac{w}{c_p}G_2(r, z) \tag{14}$$

where

$$G_1(r, z) = K_m^H\left(\frac{\partial^2}{\partial r^2} + \frac{\partial}{r\partial r} - \frac{1}{r^2}\right)u + \frac{K_m^z}{\bar{\varrho}}\frac{\partial}{\partial z}\left(\bar{\varrho}\frac{\partial u}{\partial z}\right) - u\frac{\partial u}{\partial r} - w\frac{\partial u}{\partial z} + v\left(f + \frac{v}{r}\right)$$

and

$$G_2(r, z) = -\left(u\frac{\partial w}{\partial r} + w\frac{\partial w}{\partial z} + g\right).$$

Since the terms on the right of eq. (14) are likewise known, the field of temperature was calculated by integrating (14) upward.

In the region of the updraft configuration of a severe thunderstorm where the vertical velocities are positive, the rate of change of latent heat by condensation in the ith layer (with $i = 2$, 3 or 4), $[\dot{Q}_L]_i$, is expressed as

$$[\dot{Q}_L]_i = [\dot{Q}_{Lr}]_i + [\dot{Q}_{Lz}]_i \tag{15}$$

where

$$\left.\begin{aligned} \dot{Q}_{Lr} &= -Lu\left(\frac{\partial q_s}{\partial r}\right), \\ &\text{and} \\ \dot{Q}_{Lz} &= -Lw\left(\frac{\partial q_s}{\partial z}\right). \end{aligned}\right\} \tag{16}$$

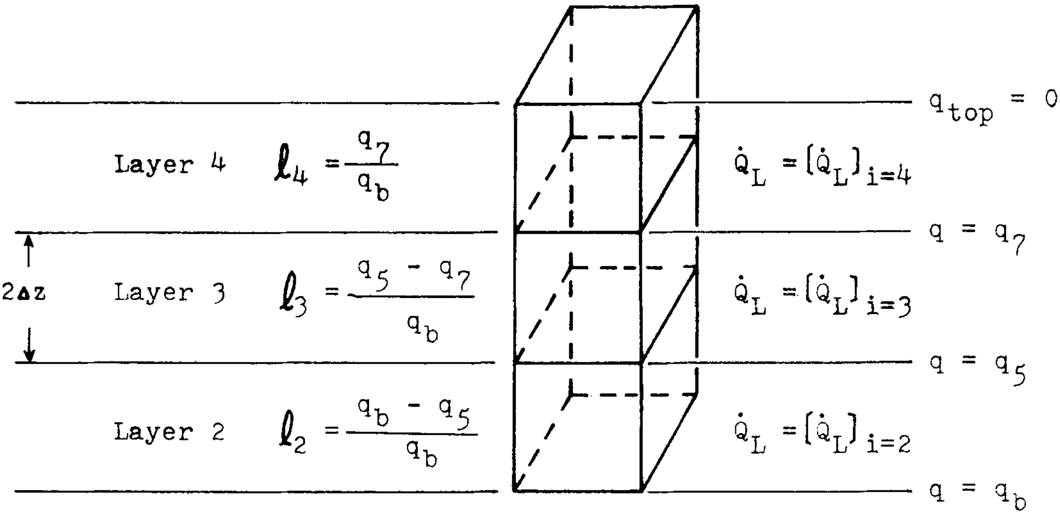

Fig. 3. A schematic representation of the "partition ratio" of water vapor condensed and the latent heat released in the ith layer, l_i and $[\dot{Q}_L]_i$, within a unit column of air.

The "partition ratio" of condensed water vapor in the ith layer

$$l_i \equiv \frac{q_{2i+1} - q_{2i-1}}{q_{\mathrm{top}} - q_{\mathrm{b}}} \tag{17}$$

was employed (see Fig. 3). In the above, q_b and q_{top} represent the specific humidity at the cloud base ($z = z_b$) and the top of the modelled storm ($z = z_t$), respectively. The "partition ratio", l_i, has a magnitude between 0 and 1. This parameter represents the ratio of water vapor condensed, per unit cross-section, in any one of the three main layers to that of a unit section extending throughout the entire updraft. It is comparable to the partition ratio of latent heat released for a tropical storm introduced by Yamasaki (1968). The boundary condition that q vanishes at the top of the modelled storm is invoked to provide the following values of $[\dot{Q}_L]_i$ for each of the three main layers

$$\left.\begin{aligned}
[\dot{Q}_L]_2 &= L\left[\frac{l_2 q_b w_4}{2\Delta z} - \frac{u_4(2-l_2)}{2}\frac{\partial q_b}{\partial r}\right] \\
[\dot{Q}_L]_3 &= L\left[\frac{l_3 q_b w_6}{2\Delta z} - \frac{u_6(2-2l_2-l_3)}{2}\frac{\partial q_b}{\partial r}\right] \\
&\text{and} \\
\dot{Q}_L]_4 &= L\left[\frac{l_4 q_b w_8}{2\Delta z} - \frac{u_8(1-l_2-l_3)}{2}\frac{\partial q_b}{\partial r}\right]
\end{aligned}\right\} \tag{18}$$

A more detailed derivation of eq. (18) is given in the Appendix. The first term on the right-hand side of each equation in (18) represents the vertical advection, and the second term the lateral advection, of latent heat. The values of l_i (with $i = 2$, 3 and 4) are given by eq. (17) and shown in Fig. 3.

3.3. *Pressures* $P(r, z)$

After obtaining the fields of vertical velocity (w) and temperature (T) within the main body of the storm's updraft configuration, the field of pressure was calculated from the radial equation of motion (1) with the form

$$\frac{\partial \ln P}{\partial r} = \frac{1}{R_d T} G_1(r, z) \tag{19}$$

by integrating inward from the outer boundary of the updraft $r = r_{lb}$ to the center $r = 0$. Here the function $G_1(r, z)$ is known which is given in Section 3.2.

In the subcloud layer of the storm ($0 \leqslant z_s \leqslant z_b$), composite moisture values, deduced from Darkow's (1969) average tornado-proximity sounding, and a set of NSSL's (National Severe Storms Laboratory) in-storm sounding (see Barnes, 1972; Henderson, 1972) provide the observational specific humidity and temperature data along the edge of the storm's updraft configura-

Table 4. *Lateral boundary values of temperature, T_r(°K), specific humidity, q_r (g kg^{-1}), pressure, p_r(mb), and density, $\bar{\varrho}$ (g cm^{-3}), along the edge of the updraft in the subcloud layer*

These values were deduced from the average tornado-proximity sounding of Darkow (1969)

z (km)	T_r (°K)	q_r (g kg^{-1})	p_r (mb)	$\bar{\varrho}$ (10^{-3} g cm^{-3})
0	301.3	18.0	1 013.3	1.172
0.1	300.3	17.0	1 001.3	1.162
0.2	299.2	16.5	989.5	1.152
0.3	298.2	16.0	977.7	1.143
0.4	297.1	15.5	966.1	1.133
0.5	296.0	15.0	954.6	1.124
0.6	295.4	14.7	943.2	1.112
0.7	294.8	14.4	931.9	1.101
0.8	294.2	14.0	920.7	1.090
0.9	293.6	13.5	909.6	1.080
1.0	293.0	13.2	898.7	1.069

tion. These data are needed for our modelling efforts and are shown in Table 4.

The field of tangential velocity component, $v_s(r, z_s)$, for the subcloud layer was generated using eqs. (7) and (8). The vertical velocity within the same layer $w_s(r, z_s)$, was extrapolated downward from the top of this layer ($z = z_b$) to the surface ($z = 0$) using the analytical expression

$$w_s(r, z_s) = w_b\left[1 - \left(\frac{z_b - z_s}{z_b}\right)^{2/3}\right]^{2/3} \tag{20}$$

Once fields of w_s were found, eq. (4) was employed to deduce the radial velocities, $u_s(r, z_s)$ within the subcloud layer.

The values of specific humidity, q_r, shown in Table 4 were used as lateral boundary conditions for q^* within the subcloud layer along the radii of $r = 10$ km and $r = 10.25$ km, respectively. The field of specific humidities, $q^*(r, z_s)$, was obtained by integrating eq. (6) inward from $r_{lb} = 10$ km to the core of the modelled storm ($r = 0$) with the aid of the generated fields u_s, v_s and w_s and the lateral boundary values of specific humidity $q_r(r_{lb}, z_s)$. Values of specific humidity q_b at the top of the subcloud layer ($z = z_b$) were obtained from the field of $q^*(r, z_s)$. These values are necessary to assess the field of temperature discussed in Section 3.2.

4. Discussion of numerical results

It is obviously impossible to justify the many assumptions of the model with sufficient confidence to expect the derived quantities to represent the detailed structure of the natural storm. On the other hand, the research is of minimal value unless such comparisons do, in fact, show that certain gross features of the natural storm are being quasi-realistically represented by the modelling equations. Various comparisons between the modelled storm and the real atmosphere will be presented to show similarities between modelled and observed responses to changes in environmental humidity conditions. The check-sounding and proximity-sounding data furnished by Darkow (1969) provide one set of "observed" source material. The proximity-sounding is representative of *environmental* conditions when severe thunderstorms subsequently occurred, and the check-sounding pertains to these cases when they did not. Both were taken within the same overall embedding synoptic environment. The other set of reference data was provided by NSSL. Specifically, on April 29, 1970 an in-storm sounding was launched from Wheatland, Oklahoma at the same time that its environmental data were being collected at Noble, Oklahoma.

Since Darkow's soundings represent a composite of many situations, only generalized relationships between the modelled product and the "typical" severe thunderstorm can be inferred. The observed meso-data of NSSL, being representative of an individual event, permit case study comparisons between the modelled and observed storm. Two parameters, in particular, will be compared. They are the "static energy differentials" between the storm and its environment, and the relative magnitudes of the latent heat releases.

4.1. *Interdependencies between the environmental moisture fields and the thermal structure of a modelled storm*

The data of Table 4 show a mean specific humidity of about 15 g kg^{-1} or a relative humidity of approximately 80% in the subcloud layer. This value under the axial-symmetric assumption pertains to all radii 10 km from the center at ground level. The analytically formulated horizontal winds (see eqs. 7 through 11) also specify the vorticity values for calculating the

Table 5. *Temperature lapse rates in the lower and middle layers given by the model calculations (column 1), Ninomiya (column 2), and Darkow (column 3)*

	Model	Ninomiya's	Darkow's
Lower layer	5.8°C km^{-1}	6.0°C km^{-1}	6.4°C km^{-1}
Middle layer	6.5°C km^{-1}	8.2°C km^{-1}	8.0°C km^{-1}

"frictionally induced" vertical velocity, $w_b(r, z_b)$. The modelling effects result in moisture convergences near the center of the updraft ($r = 0$) which increase the relative humidity by some 5% to 10% over that prescribed along the edge of the updraft configuration ($r = r_{lb}$). The interplay between the specific humidity values and the subcloud layer wind fields provide the horizontal grid of moisture and vertical velocity values at the cloud base, $z = z_b$, needed to integrate the modelling equations and assess the effects that the vertical transport of moisture has on the thermal structure of the storm. The lifting condensation level (LCL) for this case is slightly higher than 1 km and over 50% of the water vapor is contained in the layers below 500 mb. Thus, the partitioning ratio, l_i, for this particular case is approximately 50% in layer 2, 40% in layer 3 and 10% in layer 4 of the model (see Fig. 3). The calculated temperature lapse rates, γ, for layers 2 and 3 of the modelled storm are shown in Table 5 along with those deduced from the observational studies of Darkow (1969) and Ninomiya (1971). The values given by these two authors are characteristic of the storm's environment where convective activity is less vigorous than that within our modelled severe thunderstorm. This accounts for the smaller lapse rates calculated by the model since, obviously, more latent heat of condensation is released within a given area covered by a vigorous storm than for other areas of similar size within the environment.

The heavy line in Fig. 4 shows the "static energy" profile per unit mass, $E_s = C_p T + gz + Lq$, which was deduced by the model. This is to be compared with the "static energy" profile of Darkow (1968, 1969) which is representative of the "synoptic" environment. Since his proximity values provided the lateral boundary conditions for our modelling efforts, the differences in profiles are "solely" attributable to the modelling equations operating on the peripheral data.

An independent set of "static energy" profiles is given by NSSL's data (Henderson, 1972). The in-storm sounding was launched at 2233 CST, 29 April 1970 at Wheatland, Oklahoma, while the environmental sounding was taken at 2247 CST, 29 April 1970 at Noble, Oklahoma. Although the NSSL's data carries more refinements than either the profiles of Darkow or the model, the "static energy" representative of their sounding appears in good agreement with that given by the model in the lower 6 km at the same time that the "static energy" calculated from the synoptic-environmental sounding is comparing quite favorable to that of Darkow. This indicates that the model is capturing certain elements of reality with respect to the gross energy aspects of the storm vis-à-vis those of its environment.

An appreciable amount of water vapor is required from the environment to feed the subcloud layer of the storm by lateral moisture transport processes, $\varrho q^* u_s$. Magnitude values of $\varrho q^* u_s$ on the order of 10^{-3} g cm^{-2} sec^{-1} in the subcloud layer were calculated in this experiment. These are comparable to those given by Fankhauser (1965), i.e., about 4×10^{-3} g cm^{-2} sec^{-1}. Since inflow is essentially confined to the layer below the cloud base, the magnitude of this term decreases very sharply with storm height. The spatial mean of the vertical moisture flux density, $\widetilde{\varrho q w}$, at a given height, z, is given by

$$M_z \equiv \widetilde{\varrho q w} = \frac{1}{A} \int_0^{2\pi} \int_0^{r_c} (\varrho q w)\, r\, dr\, d\phi \tag{21}$$

where the cross-sectional area A is equal to 25 π km^2. Calculated values of M_z, in units of 10^{-4} g cm^{-2} sec^{-1}, at selective heights are given in Table 6 along with those of other investigators. The value reported by Auer & Marwitz (1968) was obtained from eight hailstorm occurrences in NE Colorado during the years of 1964 and 1965, and Lin & Martin (1972) computed their value from modelling experimentations at the level where comparative data are available.

The total latent heat in a unit column of air, $\dot{Q}_L^*$, was then calculated using the observed in-storm sounding of NSSL on 29 April 1970 at Wheatland, Oklahoma. The following formulation was used:

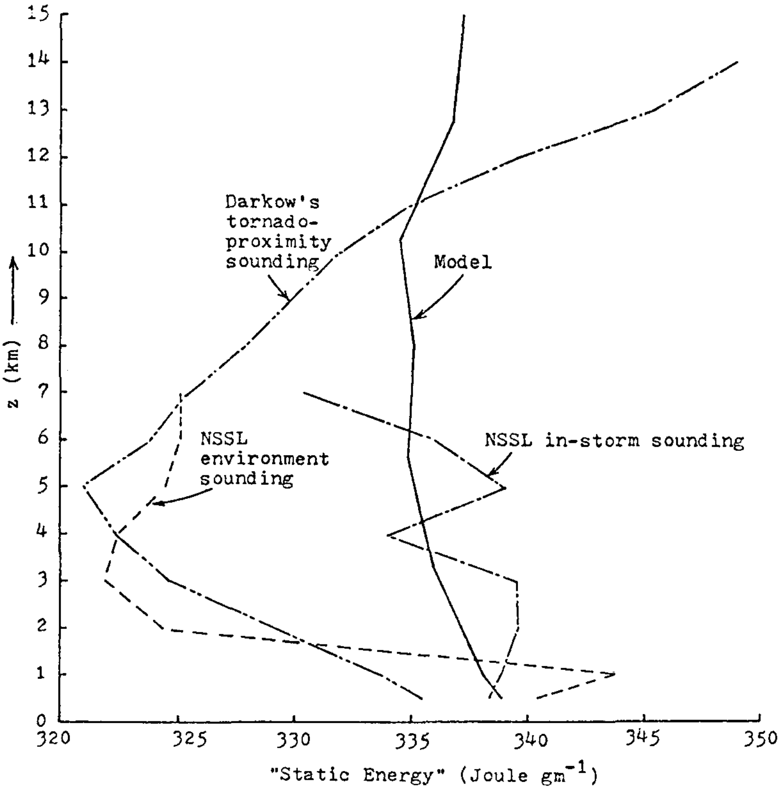

Fig. 4. "Static energy", per unit mass, obtained from our model, NSSL's in-storm and environmental soundings and Darkow's tornado-proximity sounding.

$$\dot{Q}_L^* \equiv \int_{z_b}^{z_t} \dot{Q}_L \varrho dz \approx -L \int_{z_b}^{z_t} w \frac{\partial q_s}{\partial z} \varrho dz \tag{22}$$

The term on the right of (22) can be expanded into two terms, i.e.,

$$-L \int_{z}^{z_t} w \frac{\partial q_s}{\partial z} \varrho dz = -L \int_{z_b}^{z_t} \frac{\partial(\varrho q_s w)}{\partial z} dz + L \int_{z_b}^{z_t} q_s \frac{\partial(\varrho w)}{\partial z} dz \tag{23}$$

After applying the boundary conditions that $w=0$ and $q=0$ at $z=z_t$, we arrive at the following form for $\dot{Q}_L^*$:

$$\dot{Q}_L^* \approx L(\varrho w)_{z=z_b}(q_b - \bar{q}) \tag{24}$$

where $\bar{q}$ is the mean value of saturation specific humidity with respect to height, and $(\varrho w)_{z_b}$ denotes the vertical mass flux across the cloud base.

Eq. (24) applied to the observed data of 29 April 1970 gives 8.1 Joule cm^{-2} sec^{-1} with an accompanying cloud base of 1.18 km (see Table 7, Case B). The model-generated values obtained when Darkow's check-sounding (no severe thunderstorms occurring subsequently) was used as the humidity input parameter gave a latent heat release value of 6.4 Joule cm^{-2} sec^{-1} (Case C of Table 7). This difference is quite large as reflected by the higher cloud base of 2.1 km. Presumably, a cloud base of this height is too great, in general, for the severe thunderstorm to develop. Thus, the very fact that the modelled values of Case C and the observed values of Case B differ by such a large amount (see Fig. 5) is encouraging. Next, the model-generated data based on Darkow's proximity sounding were processed to obtain a value of 7.8 Joule cm^{-2} sec^{-1} for $\dot{Q}_L^*$ (see

Table 6. *Calculated mean values of vertical moisture flux density, M_z, at selective heights*

Comparable values of M_z obtained by Lin & Martin (1972) and by Auer & Marwitz (1968) at $z = 3$ km are also shown. Units: 10^{-4} g cm^2 sec^{-1}

z (km)	Model	Lin & Martin's	Auer & Marwitz's
3.3	23.5	24.1	36.5
5.7	17.1		
8.0	11.8		
10.3	6.2		
12.7	4.1		
15.0	0.0		

Table 7 and Fig. 5, Case A) accompanied by a cloud base of 1.28 km. These compare very well with the NSSL's observed sounding data. This one case study indicates that the model is capable of discriminating between those environments which are and are not the more probable producers of severe thunderstorms through a consideration of their respective humidity fields. We would, indeed, be pleased if such comparisons were found to pertain in general—a question which will remain unanswered until contemporary in-storm and environmental sounding data for other situations become available for comparative purposes.

Thus, although the modelled results are fraught with many assumptions, these experiments at least would seem to indicate that the model is capable of delineating certain responses between the severe thunderstorm and its environment which trend in the same direction as those found in the real world. Whether or not the absolute magnitude range of $\dot{Q}_L^*$ which we presented constitutes a meaningful delineation between the highly probable and the seldom occurring severe thunderstorm is left for time to tell.

Table 7. *Calculated total latent heat release, $\dot{Q}_L^*$, in a unit column of air in the center of the updraft when Darkow's proximity-sounding defined the environmental humidities (Case A), for the observed NSSL's in-storm sounding (Case B), and when Darkow's check-sounding characterized the environmental humidities (Case C)*

Case	A	B	C
Mean R.H. (%)	80	85	60
LCL (km)	1.28	1.18	2.10
$\dot{Q}_L^*$ (Joule cm^{-2} sec^{-1})	7.8	8.1	6.4

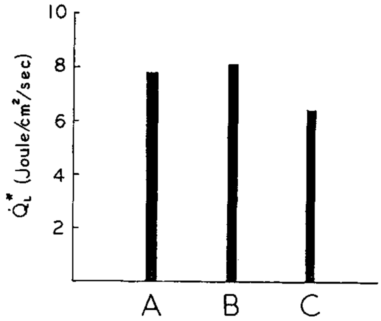

Fig. 5. Calculated total latent heat release, $\dot{Q}_L^*$, in a unit column of air in the center of the updraft when Darkow's proximity sounding defined the environmental humidities (*A*), for the observed NSSL's in-storm sounding (*B*), and when Darkow's check sounding characterized the environmental humidities (*C*). Units: Joule cm^{-2} sec^{-1}.

In order to examine the influence of various "partition ratios" of condensed water vapor, l_i, in each layer on the thermal structure of the model storm, other numerical experiments with different values of l_i were also made. Results show that the calculated temperature field within the main body of the storm's updraft configuration is quite sensitive to the vertical moisture gradients, $\delta q_s/\delta z$. The most suitable way to form a "warm-core" structured storm at mid-altitudes (supported by many observational studies, e.g., Ninomiya, 1971; Henderson, 1972, etc.) is to condense a larger amount of water vapor in the lower layers of the severe thunderstorm.

4.2. *The role of eddy diffusion processes within the subcloud layer*

Eq. (6) was used to calculate the moisture field of the subcloud layer using the same boundary conditions and parameters employed in Case A. However, the diffusion coefficients were allowed to vary among the experiments until a wide extreme of values was tested.

One experiment assumed that both $K_w^H = K_w^z = 0$, i.e., no diffusion processes are operative. Specific humidities under this assumption were calculated for each grid point within the subcloud layer by integrating eq. (6) inward from the outer boundary, $r = r_{lb}$, to the center. The lateral boundary condition of q^* was specified as previously discussed in Section 4.1, and $\delta q^*/\delta r$ was set equal to zero at $z = 0$. Under these conditions, the specific humidity at the core of the storm ($r = 0$) reached its saturation value immediately above the ground. Such low cloud bases for a severe thunderstorm do not fit either the observational evidence of Case B or the model deduced values of Case A.

In another experiment only the vertical mixing was assumed to operate, i.e., $K_w^H = 0$ and $K_w^z = 10^6$ cm² sec⁻¹. The low-level saturation in the modelled subcloud layer was found to be more extreme than they were when the conditions $K_w^H = K_w^z = 0$ were imposed. Other calculations such as cloud-base heights, for example, were quite similar in both cases.

Next, only the horizontal mixing component was permitted to operate, i.e., $K_w^H = 10^{10}$ cm² sec⁻¹ and $K_w^z = 0$. Somewhat surprisingly, a cloud-base height quite close to that found under Cases A and B in Table 7 was found.

Finally, both lateral and vertical mixing were permitted to operate when K_w^H was reduced for a factor of ten with $K_w^z = 10^6$ cm² sec⁻¹ remaining the same as in the other experiments. The calculated lateral moisture gradients were found to be considerably larger than those reported for the observed storm (Case B of Table 7).

Based on the above experimental deductions and observational comparisons, we conclude that:

(*a*) Subcloud mixing by turbulent processes exerts an important influence on the thermal structure of the updraft as well as the moisture distribution of the subcloud layer.

(*b*) Horizontal mixing processes play a more dominant role than the vertical ones in distributing the moisture of the subcloud layer throughout the main body of the storm.

(*c*) Values of $K_w^H = 10^{10}$ cm² sec⁻¹ and $K_w^z = 10^6$ cm² sec⁻¹ provide results which best tune our modelling experiments to known characteristics of the natural cloud.

(*d*) Magnitude ranges of K_w^H and K_w^z appear to be highly dependent on the specific cloud model under consideration.

5. Summary and conclusions

A four-layer, non-entraining model of a severe thunderstorm with an axial-symmetric rotating updraft is devised to study various aspects of its dynamic and thermodynamic properties. In particular, some effects that low-level moisture fields and their vertical gradients exert on the internal thermal structure of the severe thunderstorm are discussed.

One set of sensitivity studies was performed using typical moisture gradients found in association with observed severe thunderstorms subsequently developing as input data to the model. Another experiment treated those moisture gradients within the same synoptic area as the first set and for which *no* subsequent storm did develop. Finally, the horizontal and vertical diffusivities for water vapor were allowed to vary.

The results indicate that:

(*a*) The vertical moisture gradients within a storm's updraft are highly correlated with the vertical moisture flux across the cloud base in response to surface humidities, lowlevel flow patterns and terrain features which encourage moisture convergence.

(*b*) The turbulent mixing of water vapor in the subcloud layer plays an important role in determining the vertical moisture distribution of the updraft. Horizontal mixing, in particular, constitutes the more effective mixing process.

(*c*) The warm-core structured storm at mid-altitudes signifies that much of the water vapor available to the storm is concentrated in the lower layers of the atmosphere.

Certain climatic studies which might be worthy of undertaking can also be inferred from these modelling experiments. Among these are (1) correlations between the frequency of severe thunderstorm occurrences and spatial-averaged environmental humidities, (2) correlations between observed cloud-base heights within an area and the probability of subsequent severe thunderstorm occurrences, and (3) the frequency of severe thunderstorms as a function of terrain induced horizontal convergences.

Acknowledgements

This research was supported by the Atmospheric Sciences Section, National Science Foundation, under Grants GA-26029 and GA-26029A1.

The authors wish to thank Professor D. E. Martin and Dr G. V. Rao of Saint Louis University for their many constructive suggestions and comments throughout the course of this study. Appreciation is also extended to Mrs Frances Brummell for typing the manuscript.

APPENDIX

The treatment of latent heat released by cumulus convection

In a "pseudo" adiabatic process, the release of latent heat of condensation, per unit mass of air during a unit time, in the ith layer of the storm's updraft is given by

$$[\dot{Q}_L]_i = -L\left(\frac{dq_s}{dt}\right)_{2i} \tag{A-1}$$

An expansion of the right-hand term produces

$$[\dot{Q}_L]_i = [\dot{Q}_{Lr}]_i + [\dot{Q}_{Lz}]_i$$

where

$$\left.\begin{aligned} \dot{Q}_{Lr} &= -Lu\left(\frac{\partial q_s}{\partial r}\right) \\ \dot{Q}_{Lz} &= -Lw\left(\frac{\partial q_s}{\partial z}\right) \end{aligned}\right\} \tag{A-2}$$

and $i = 2$, 3 or 4.

Integrating the component $\dot{Q}_{Lz}$ with respect to height from the top of the subcloud layer ($z = z_b$) to the upper boundary of the modelled storm ($z = z_t$), see Fig. 1, gives

$$\int_{z_b}^{z_t} \dot{Q}_{Lz}\,dz = \int_{z_b}^{z_5} \dot{Q}_{Lz}\,dz + \int_{z_5}^{z_7} \dot{Q}_{Lz}\,dz + \int_{z_7}^{z_t} \dot{Q}_{Lz}\,dz$$

$$= \{[\dot{Q}_{Lz}]_2 + [\dot{Q}_{Lz}]_3 + [\dot{Q}_{Lz}]_4\}\,2\Delta z$$

with

$$\left.\begin{aligned} [\dot{Q}_{Lz}]_2 &= -Lw_4\frac{(q_5 - q_b)}{2\Delta z} = Lw_4 S_2 \\ [\dot{Q}_{Lz}]_3 &= -Lw_6\frac{(q_7 - q_5)}{2\Delta z} = Lw_6 S_3 \\ &\text{and} \\ [\dot{Q}_{Lz}]_4 &= -Lw_8\frac{(q_{top} - q_7)}{2\Delta z} = Lw_8 S_4 \end{aligned}\right\} \tag{A-3}$$

In the above

$$S_i = \frac{q_{2i-1} - q_{2i+1}}{2\Delta z} \tag{A-4}$$

From eq. (A-4), we define the value of S_{tot} as

$$S_{tot} \equiv \sum_{i=2}^{4} S_i = \frac{q_b - q_{top}}{2\Delta z} \tag{A-5}$$

Since the saturation specific humidity, in general, decreases exponentially with height, it appears reasonable to assume that the value of q_{top} in eq. (A-5) is zero so that

$$S_{tot} = \frac{q_b}{2\Delta z} \tag{A-6}$$

For convenience, "partition ratio" of water vapor condensed in the layer, l_i, is introduced, i.e.

$$l_i \equiv \frac{S_i}{S_{tot}} \tag{A-7}$$

as shown in Fig. 3.

With the aid of eqs. (A-6) and (A-7), we obtain

$$S_i = \frac{l_i q_b}{2\Delta z} \tag{A-8}$$

Upon combining eqs. (A-4) and (A-8), it gives

$$l_i = \frac{q_{2i-1} - q_{2i+1}}{q_b} \tag{A-9}$$

and

$$q_{2i+1} = q_{2i-1} - q_b l_i \tag{A-10}$$

From eqs. (A-9) and (A-10), we have

$$\left.\begin{aligned} &l_2 = \frac{q_b - q_5}{q_b}, \quad l_3 = \frac{q_5 - q_7}{q_b} \\ &l_4 = \frac{q_7}{q_b}, \quad q_5 = q_b(1 - l_2) \\ &\text{and} \\ &q_7 = q_b(1 - l_2 - l_3) \end{aligned}\right\} \tag{A-11}$$

Substituting (A-11) into (A-3) yields

$$\left.\begin{aligned}[\dot{Q}_{Lz}]_2 &= \frac{Lw_4 q_b l_2}{2\Delta z}\\ [\dot{Q}_{Lz}]_3 &= \frac{Lw_6 q_b l_3}{2\Delta z}\\ \text{and}\\ [\dot{Q}_{Lz}]_4 &= \frac{Lw_8 q_b l_4}{2\Delta z}\end{aligned}\right\} \qquad \text{(A-12)}$$

On the other hand, values of saturation specific humidity at even levels ($2i$) are linearly interpolated based on the relationship

$$q_{2i} = \frac{q_{2i+1} + q_{2i-1}}{2}$$

to give

$$\frac{\partial q_{2i}}{\partial r} = \frac{1}{2}\left(\frac{\partial q_{2i+1}}{\partial r} + \frac{\partial q_{2i-1}}{\partial r}\right) \qquad \text{(A-13)}$$

Combining (A-2), (A-11) and (A-13) yields

$$\left.\begin{aligned}[\dot{Q}_{Lr}]_2 &= -Lu_4 \frac{(2-l_2)}{2}\frac{\partial q_b}{\partial r}\\ [\dot{Q}_{Lr}]_3 &= -Lu_6 \frac{(2-2l_3-l_3)}{2}\frac{\partial q_b}{\partial r}\\ \text{and}\\ [\dot{Q}_{Lr}]_4 &= -Lu_8 \frac{(1-l_2-l_3)}{2}\frac{\partial q_b}{\partial r}\end{aligned}\right\} \qquad \text{(A-14)}$$

After inserting (A-12) and (A-14) into (A-2), we finally arrive at the following parameterized forms of $[\dot{Q}_L]_i$ in layers $i = 2$, 3 and 4, respectively:

$$\left.\begin{aligned}[\dot{Q}_L]_2 &= L\left[\frac{l_2 w_4 q_b}{2\Delta z} - \frac{u_4(2-l_2)}{2}\frac{\partial q_b}{\partial r}\right]\\ [\dot{Q}_L]_3 &= L\left[\frac{l_4 w_6 q_b}{2\Delta z} - \frac{u_6(2-2l_3-l_3)}{2}\frac{\partial q_b}{\partial r}\right]\\ [\dot{Q}_L]_4 &= L\left[\frac{l_4 w_8 q_b}{2\Delta z} - \frac{u_8(1-l_2-l_3)}{2}\frac{\partial q_b}{\partial r}\right]\end{aligned}\right\} \qquad \text{(A-15)}$$

The above expressions for $[\dot{Q}_L]_i$ were used to assess the release of latent heat of condensation by water vapor within the storm's updraft configuration throughout this study.

REFERENCE

Ackerman, B. 1967. The nature of the meteorological fluctuations in clouds. *J. Appl. Meteor. 6*, 61–71.

Auer, A. H., Jr & Sand, W. 1966. Updraft measurements beneath the base of cumulus and cumulonimbus clouds. *J. Appl. Meteor. 5*, 461–466.

Auer, A. H., Jr & Marwitz, J. D. 1968. Estimates of air and moisture flux into hailstorms on high plains. *J. Appl. Meteor. 7*, 196–198.

Barnes, S. L. 1972. Morphology of two tornadic storms; an analysis of NSSL data on April 30, 1970. Preprint, 15th Radar Meteorology Conference. *Amer. Meteor. Soc.*, 69–76.

Bates, F. C. 1961. The Great Plains squall-line thunderstorm—a model. Ph.D. Dissertation, St. Louis Univ., 164 pp. University Microfilms, Ann Arbor, Mich. No. 61-6455.

Bates, F. C. 1967*a*. On the structure and mechanics of the severe thunderstorm. St. Louis Univ. (Unpublished manuscript.)

Bates, F. C. 1967*b*. A major hazard to aviation near severe thunderstorms, 36 pp. (Unpublished manuscript.)

Baxter, T. L. 1971. A thunderstorm forecast technique derived from modeling considerations. Preprints of papers, 7th Conference on Severe Local Storms, 13–16, American Meteorological Society.

Beebe, R. G. & Bates, F. C. 1955. A mechanism for assisting in the release of convective instability. *Mon. Wea. Rev. 83*, 1–10.

Bonner, W. D. 1966. Case study of thunderstorm activity in relation to the low-level jet. *Mon. Wea. Rev. 94*, 167–178.

Braham, R. R. 1952. The water and energy budgets of the thunderstorm and their relation to thunderstorm development. *J. Meteor. 9*, 227–242.

Brown, R. A. & Crawford, K. C. 1972. Doppler radar evidence of severe storm high-reflectivity cores acting as obstacles to airflow. Preprint 15th Radar Meteor. Conference. *Amer. Meteor. Soc.* 16–21.

Browning, K. A., Jr. 1964. Airflow and precipitation trajectories within severe local storms which travel to the right of the winds. *J. Atmos. Sci. 21*, 634–639.

Browning, K. A., Jr. 1965*a*. The evolution of tornadic storms. *J. Atmos. Sci. 22*, 664–668.

Browning, K. A., Jr. 1965*b*. Some inferences about the updraft within a severe local storm. *J. Atmos. Sci. 22*, 669–677.

Browning, K. A., Jr & Donaldson, R. J. 1963. Air flow and structures of a tornado storm. *J. Atmos. Sci. 20*, 533–545.

Browning, K. A., Jr & Ludlam, F. H. 1962. Airflow in convective storms. *Quart. J. Roy. Meteor. Soc. 88*, 117–135.

Byers, H. R. & Braham, R. R. 1949. The thunderstorm, U.S. Government Printing Office, Washington, D.C. 287 pp.

Charba, J. & Sasaki, Y. 1971. Structure and movement of the severe thunderstorm of 3 April 1964 as revealed from radar and surface mesonetwork data analysis. *J. Meteor. Soc. Japan*, 191–214.

Charney, J. C. & Eliassen, A. 1964. On the growth of the hurricane depression. *J. Atmos. Sci. 21*, 68–75.

Darkow, G. L. 1968. The total energy environment of severe storms. *J. Appl. Meteor. 7*, 199–205.

Darkow, G. L. 1969. An analysis of over sixty tornado proximity soundings. Preprint, 6th Conference on Severe Local Storms. *Amer. Meteor. Soc.*, 182–183.

Donaldson, R. J., Jr. 1962. Radar observations of a tornado thunderstorm in vertical section. Natl. Severe Storms Project Rep. No. 8, 21 pp.

Doswell, C. A. & Tegtmeier, S. A. 1972. Rotating clouds at Norman, Oklahoma. *Bull. Amer. Meteor. Soc. 53*, 1180.

Fankhauser, J. C. 1965. Water budget considerations in an extensive squall-line development. Tech. Note 4-NSSL-25, 28 pp. U.S. Weather Bureau, Washington, D.C.

Fankhauser, J. C. 1966. Some physical and dynamical aspects of singular cumulonimbus observed by instrumented aircraft and radar. Proc. Twelfth Conf. Radar Meteor., Boston. *Amer. Meteor. Soc.*, 405–413.

Fankhauser, J. C. 1971. Thunderstorm-environment interactions determined from aircraft and radar observations. *Mon. Weath. Rev. Wash. 99*, 171–192.

Fitzgerald, D. R. & Valovein, F. 1964. High altitude observations of the development of a tornado producing thunderstorm. A paper presented at the National Conference on the Physics and Dynamics of Clouds. AMS, 24–26, March 1964, Chicago, Ill.

Fujita, T. & Byers, H. R. 1962. Model of a hail cloud as revealed by photogrammetric analysis. *Nubila 5*, 85–105.

Fujita, T. & Grandoso, H. 1968. Split of a thunderstorm into anticyclonic and cyclonic storms and their motion as determined from numerical model experiments. *J. Atmos. Sci. 25*, 416–439.

Henderson, J. H. 1972. A detailed description of the internal structure of a thunderstorm. Preprint, 15th Radar Meteor. Conference, *Amer. Meteor. Soc.*, 61–68.

Hudson, H. R. 1971. On the relationship between horizontal moisture convergence and convective cloud formation. *J. Appl. Meteor. 10*, 755–762.

Koschielski, A. 1967. The Black Hills tornado of 23 July 1966. Fifth Conference on Severe Local Storms, pp. 226–228. American Meteorological Society.

Kuo, H. L. 1965. On formation and intensification of tropical cyclones through latent heat release by cumulus convection. *J. Atmos. Sci. 22*, 40–63.

Lin, Y. J. & Martin, D. E. 1971. On diagnostic studies of a steady axial-symmetric severe local thunderstorm with rotational updrafts. Preprints of papers, 7th Conference on Severe Local Storms, pp. 262–267. American Meteorological Society.

Lin, Y. J. & Martin, D. E. 1972. Further study of the severe storm with a rotating updraft configuration. *Tellus 24*, 216–228.

Liu, J. Y. & Orville, H. D. 1969. Numerical modeling of precipitation and cloud shadow effects on mountain-induced cumuli. *J. Atmos. Sci. 26*, 1283–1298.

Malkus, J. S. & Williams, R. T. 1963. On the interactions between severe storms and large cumulus clouds. *Meteor. Monogr. 5*, 59–64.

Marwitz, J. D. 1972*a*. The structure and motion of severe hailstorms. Part I: Supercell storms. *J. Appl. Meteor. 11*, 166–179.

Marwitz, J. D. 1972*b*. The structure and motion of severe hailstorms. Part II: Multi-cell storms. *J. Appl. Meteor. 11*, 180–188.

Marwitz, J. D. 1972*c*. The structure and motion of severe hailstorms. Part III: Severely sheared storms. *J. Appl. Meteor. 11*, 189–201.

Marwitz, J. D. 1972*d*. Trajectories within the weak echo regions of hailstorms. Preprint, 15th Radar Meteor. Conference, *Amer. Meteor. Soc.*, 53–56.

Miller, R. C. 1972. Notes on analysis and severe-storm forecasting procedures of the Air Force Global Weather Center. Air Weather Service, Tech. Rept. No. 200, 180 pp.

Newman, W. R. 1972. The relationship between horizontal moisture convergence and severe storm occurrences. Res. Rept. No. OURI-1828-72-2, University of Oklahoma. 54 pp.

Newton, C. W. 1966. Circulations in large sheared cumulonimbus. *Tellus 18*, 699–713.

Ninomiya, K. 1971. Dynamical analysis of outflow from tornado-producing thunderstorms as revealed by ATS III pictures. *J. Appl. Meteor. 10*, 275–294.

Ogura, Y. 1963. The evolution of a moist convective element in a shallow, conditionally unstable atmosphere: a numerical calculation. *J. Atmos. Sci. 20*, 407–424.

Orville, H. D. & Sloan, L. J. 1970. A numerical simulation of the life history of a rainstorm. *J. Atmos. Sci. 27*, 1148–1159.

Rhyne, R. H. & Steiner, R. 1964. Power spectral measurement of atmospheric turbulence in severe storms and cumulus clouds. NASA TND-2469, NASA, Washington, D.C.

Rosenthal, S. L. 1970*a*. Experiments with a numerical model of tropical cyclone development—some effects of radial resolution. *Mon. Weath. Rev. Wash. 98*, 106–120.

Rosenthal, S. L. 1970*b*. A circularly symmetric primitive equation model of tropical cyclone development containing an explicit water vapor cycle. *Mon. Weath. Rev. Wash. 98*, 643–663.

Sasaki, Y. 1966. Structure and motion of convective systems under influences of boundary layer. Tech. Rept. No. ARL-1523-1. Oklahoma University Atm. Res. Ins. 23 pp.

Sasaki, Y., Lewis, J. M., Chen, T. S., French, L. & Harmon, J. 1967. Dynamical forecasting of severe local storms. Tech. Rept. Univ. of Oklahoma Res. Inst. 20 pp.

Schlesinger, R. E. 1971. A numerical model of deep moist convection: The influence of ambient conditions and internal physical mechanisms. Ph.D. dissertation, University of Wisconsin. 207 pp.

Steiner, R. & Rhyne, R. H. 1962. Some measured characteristics of severe storm turbulence. NSSP Rep. No. 10, U.S. Weather Bureau, Washington, D.C.

Takeda, T. 1971. Numerical simulation of a precipitating convective cloud: The formation of a "long-lasting" cloud. *J. Atmos. Sci. 28*, 350–376.

U.S. Weather Bureau. 1965. Forecasting tornadoes and severe thunderstorms. Forecasting guide No. 1. Washington, D.C. 35 pp.

Yamasaki, M. 1968. A tropical cyclone model with parameterized vertical partition of released latent heat. *J. Meteor. Soc. Japan 46*, 202–214.

ВЛИЯНИЕ РАСПРЕДЕЛЕНИЯ ВЛАЖНОСТИ В ПОДОБЛАЧНОМ СЛОЕ НА ТЕРМИЧЕСКУЮ СТРУКТУРУ МОЩНОГО КУЧЕВОГО ОБЛАКА

Четырехуровенная, осесимметричная, стационарная модель мощного кучевого облака с вращением восходящего потока и в пренебрежении перемешиванием используется для изучения влияния влажности на нижних уровнях на термическую и динамическую структуру конвекции. Модель является третьей в серии из трех моделей, разработанных в Университете Сент-Луиса. Она отличается от двух других, разработанных Лином и Мартином (1971, 1972) тем, что влажность скорее задается как входной параметр, а не получается в модели. Все три модели прошли проверку на внутреннюю согласованность, так что любая может быть использована для воспроизведения в общих чертах искомых элементов в зависимости от имеющихся эмпирических данных. Комбинация наблюдаемых и воспроизводимых данных в восходящем потоке моделируемого конвективного облака использовалась для оценки: 1) вертикальных скоростей по уравнению неразрывности, 2) распределения влажности в подоблачном слое по уравнению неразрывности для водяного пара, 3) поля давления из радиального уравнения движения, 4) поля температуры путем использования термодинамического уравнения энергии, 5) потоков влажности, выделения скрытого тепла и статической энергии с помощью пп. 1–4. Результаты показывают, что существенный процент выделения скрытого тепла в облаке должен быть сосредоточен в нижней части атмосферы для того, чтобы могла поддерживаться теплая центральная часть. Найдено, что относительная влажность окружающего воздуха на нижнем уровне является хорошим индикатором развития мощной кучевой конвекции. Для моделируемых и наблюдаемых кучевых облаков сравниваются «дифференциалы статической энергии» с целью проиллюстрировать некоторое согласие между моделируемым и естественными физическими процессами.